Diffusion Modeling in a Generic Clay Repository: Impacts of Heterogeneity and Electro-Chemical Process

Fuel Cycle Research & Development

Prepared for

U.S. Department of Energy
Used Fuel Disposition

Marco Bianchi
Hui-Hai Liu
Jens Birkholzer

Lawrence Berkeley National Laboratory

May, 2012

FCRD-UFD-2012-000127

FCT Quality Assurance Program Document Revision 1 08/19/2011

Appendix E
FCT Document Cover Sheet

Name/Title of Deliverable/Milestone	Diffusion Modeling in a Generic Clay Repository: Impacts of Heterogeneity and Electro-Chemical Process
Work Package Title and Number	Generic Disposal System Level Modeling - LBNL FT-12LB080803
Work Package WBS Number	1.02.08.08
Responsible Work Package Manager	Hui-Hai Liu (Name/Signature)
Date Submitted	5/25/2012
Quality Rigor Level for Deliverable/Milestone	☐ QRL-3 ☐ QRL-2 ☐ QRL-1 ☐ Nuclear Data ☒ N/A*
This deliverable was prepared in accordance with	Lawrence Berkeley National Laboratory *(Participant/National Laboratory Name)*

QA program which meets the requirements of
☒ DOE Order 414.1 ☐ NQA-1-2000 ☐ Other

This Deliverable was subjected to:

☐ Technical Review ☐ Peer Review

Technical Review (TR)

Review Documentation Provided
- ☐ Signed TR Report or,
- ☐ Signed TR Concurrence Sheet or,
- ☐ Signature of TR Reviewer(s) below

Peer Review (PR)

Review Documentation Provided
- ☐ Signed PR Report or,
- ☐ Signed PR Concurrence Sheet or,
- ☐ Signature of PR Reviewer(s) below

Name and Signature of Reviewers

_____ _____

_____ _____

_____ _____

*__NOTE__ *In some cases there may be a milestone where an item is being fabricated, maintenance is being performed on a facility, or a document is being issued through a formal document control process where it specifically calls out a formal review of the document. In these cases, documentation (e.g., inspection report, maintenance request, work planning package documentation or the documented review of the issued document through the document control process) of the completion of the activity along with the Document Cover Sheet is sufficient to demonstrate achieving the milestone. QRL for such milestones may be also be marked*

This page is intentionally blank.

SUMMARY

The dominant transport mechanism of chemical species at locations away from the excavation damaged zone in clay-rich geological formations is diffusion, which is influenced by factors such as the heterogeneity of the diffusive parameters and electrochemical processes. The latter are the results of interactions between chemical species in solutions and charged surfaces of clay minerals. Numerical models for performance assessment (PA) of clay repositories need to consider these factors in order to correctly simulate the long term transport behavior. This report describes a study aimed at developing an improved approach for modeling diffusive transport in clay-rich geological formations. In particular, we proposed a rigorous and practical framework to account for heterogeneity of the diffusive parameters. Expressions for upscaling the diffusion coefficient were developed based on the analogy between diffusion and water flow in saturated heterogeneous porous media. Comparisons between numerical and analytical values of the equivalent upscaled diffusion coefficient showed that conventional stochastic and power-averaging upscaling methods can be effectively applied to upscale laboratory-scale D measurements for large scale numerical models. We also evaluated a simplified model to incorporate the electrochemical impact on diffusion in clay-rich formations. Results indicate a good match between analytical predictions from this model and experimental data for different chemical species from the Opalinus Clay (OPA) and Callovo-Oxfordian Argillites (COx). By fitting the model to the experimental data, we found that the electrical potential in the OPA and in the COx formations is equal to about -11 mV and 23 mV, respectively. Analogously, for both geological formations, the optimal values for the macropore water fraction were found to be equal zero. This result suggests that the entire pore space is subject to electrochemical processes. Future work will focused on understanding the physical meaning and uncertainties of these parameters. We also plan to develop a framework for estimating the uncertainty of upscaled diffusion coefficients and integrating this research activity with the system-level clay model developed by ANL by providing inputs (upscaled parameter values and related uncertainty) to the ANL model.

CONTENTS

FIGURES

TABLES

ACRONYMS

COx	Callovo-Oxfordian
DDL	Diffusive Double Layer
HTO	Tritiated water
MA	Mean Absolute Error
OPA	Opalinus Clay
PA	Performance assessment
RMSE	Root Mean Square Error

1. INTRODUCTION

Because of their low permeability and high retention capacity for radionuclides, clay-rich geological formations have been evaluated as potential long-term deep geological repositories for high-level nuclear waste. Examples of these formations include the Callovo-Oxfordian Argillites at the Bure site in France (ANDRA 2005), the Toarcian Argillites at the Tournemire site in France (Patriarche et al. 2004), the Opalinus Clay at the Mont Terri site in Switzerland (Bossart et al. 2001) and the Boom Clay at the Mol site in Belgium (Barnichon and Volckaert 2003). In the U.S., clay-rich formations of different ages are widely distributed especially in central and eastern part of the country (Figure 1).

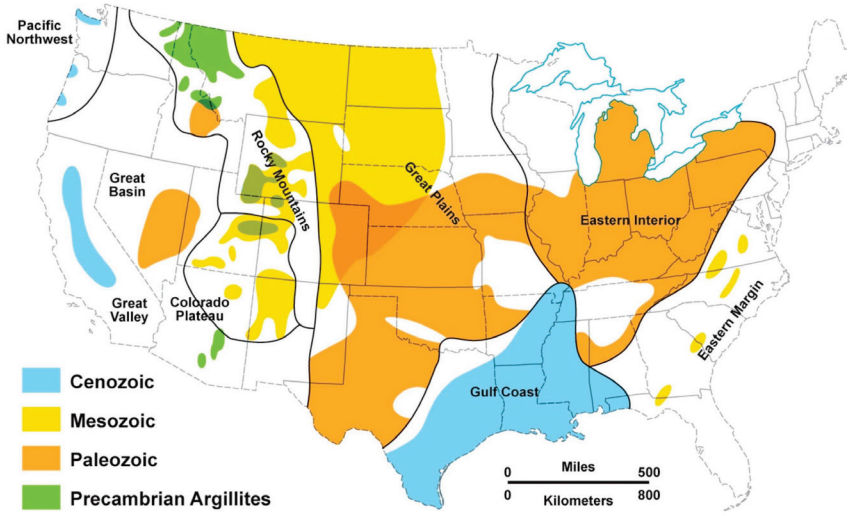

Figure 1. Distribution of the clay-rich formations in the USA (adapted from Gonzales and Johnson 1984)

Since diffusion is the dominant transport mechanism in clay, several previous studies collected and reported datasets of diffusive parameters from these formations (e.g., Aertsen et al. 2004; Patriarche et al. 2004; Van Loon et al. 2004a and 2004b; Descostes et al. 2008; Jougnot et al. 2009, Appelo et al. 2010). A summary of the diffusion parameters collected in clay-rock formations available in the literature was presented by Zheng et al. (2011). The analysis of these data reveals that the diffusion coefficient (*D),* is a heterogeneous property with variations that can be of about two orders of magnitude within the same formation or stratigraphic sequence (Figure 2). Experimental results also show that *D* is anisotropic (Figure 3) since values measured along directions parallel to sedimentary bedding are about two to four times larger than those measured perpendicularly (Van Loon et al. 2004a and 2004b; García-Gutiérrez et al. 2006; García-Gutiérrez et al. 2008; Samper et al. 2008). Numerical models for performance assessment (PA) of clay repositories need to consider the heterogeneity of the diffusive parameters in order to correctly simulate the long term transport behavior at the macro and formation scale. In particular, because the support scale of the *D* measurements is small, since this parameter is usually estimated with laboratory diffusion tests through centimetric-to-decimetric rock samples (e.g., Samper et al. 2008; Cormenzana et al. 2008), upscaling is required to use these data in large-scale PA models.

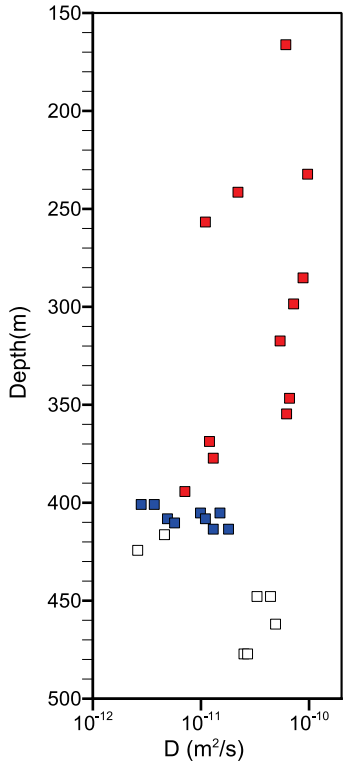

Figure 2. *D* of tritiated water (HTO) as a function of depth in samples collected in the Callovo-Oxfordian argillites and in the Oxfordian limestones (France). Red squares: Oxfordian limestones; blue squares: base of the Oxfordian limestones; white squares: Callovo-Oxfordian argillites. Data is from Descostes et al. (2008).

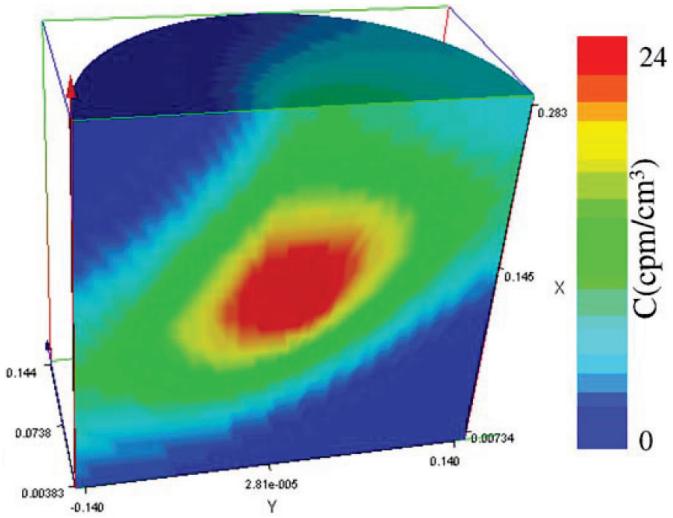

Figure 3. Diffusion experiments in a sample of the Opalinus Clay formation showing the effect of anisotropy of the diffusion coefficient (García-Gutiérrez et al. 2006). The sample is cylindrical with a diameter of 30 cm. Colors represent the concentration distribution of tritiated water HTO in the sample.

It is well known that in clay-rich formations, due to interactions between chemical species in solutions and charged mineral surfaces, electrochemical processes have a significant effect on diffusion (e.g., Zheng et al. 2011). However, a practical approach to incorporating this effect into the related PA models is still lacking. Resolving this issue is critical for reducing the uncertainty in modeling diffusion processes and increasing scientific defensibility of the related PA models.

The objective of this work is to develop an improved approach to dealing with impacts of heterogeneity and electrochemical processes and associated uncertainties. This work addresses Features, Events and Processes FEP 2.2.09, Chemical Process—Transport (shale), which has been ranked *medium* in importance, as listed in Table 7 of the Used Fuel Disposition Campaign Disposal Research and Development Roadmap (FCR&D-USED-2011-000065 REV0) (Nutt 2011). This report presents the progress that has been made in the FY12. Section 2 reports study results of upscaling D in anisotropic and heterogeneous clay-rock formations. Section 3 discusses the evaluation of a new model to handle the impacts of electrochemical processes on diffusion, which was developed and reported in the FY11 report (Zheng et al. 2011). Section 4 presents concluding remarks and discusses future work.

2. EQUIVALENT DIFFUSION COEFFICIENT OF CLAY-RICH GEOLOGICAL FORMATIONS: COMPARISON BETWEEN NUMERICAL AND ANALYTICAL ESTIMATES

In the hydrogeological literature, the upscaling problem has been mostly investigated with a focus on hydraulic conductivity (see the comprehensive reviews of Wen and Gómez-Hernandez 1996; Renard and de Marsily 1997 and Sanchez-Vila et al. 2006). In the context of solute transport, analytical expressions were mostly developed to relate macrodispersivity to the spatial correlation structure of hydraulic conductivity (e.g., Gelhar et al. 1979; Gelhar and Axness 1983; Dagan 1984; Neuman et al. 1987; Dagan 1988; Rubin 1990; Zhang and Neumann 1996; Zhou and Selim 2003; Frippiat and Holeyman 2008 and references therein). In general, the problem of upscaling diffusive parameters has not received much attention by the scientific community. Among the few works about this topic, Huysmans and Dassargues (2007) proposed analytical expressions for the equivalent pore diffusion coefficient and the equivalent accessible porosity. The problem was formulated in transient state and the equivalent D was found to be equal to the power average of the pore diffusion coefficients of single layers for short times and to the harmonic average for long times. Their analysis is however limited to a 1-D layered porous medium. Dai et al. (2007) derived an expression for the equivalent matrix diffusion coefficient in fractured rocks and found that it is a function of the geometric mean, variance and integral scale of the laboratory measured D values and the size of the domain of interest. This expression is valid for 1-D isotropic system and when the variance of the D distribution is smaller than one. At a much smaller scale, Churakov and Gimmi (2011) proposed a two-step approach for upscaling D from the nanometric pore scale to the micrometer scale. With respect to previous studies, the novelty of our study is that it addresses the issue of upscaling D in an anisotropic and heterogeneous three-dimensional saturated system. The diffusion coefficient D is assumed to be a spatial random variable, allowing us to apply upscaling expressions based on statistics of the D field. These expressions, originally developed for upscaling hydraulic conductivity (Gelhar and Axness 1983; Ababou 1991; Desbarats 1992; Indelmann and Abramovich 1994; De Wit 1995), are here applied in the context of diffusive transport on the basis of the analogy between the physical processes of steady-state groundwater flow and diffusion in porous media.

2.1 Review of factors controlling the spatial variability of D in clay-rich formations

Solute transport in porous media is controlled by subsurface heterogeneity at various scales. However, the heterogeneity of D has been ignored in hydrogeological models compared to hydraulic conductivity and dispersive parameters. The spatial variability of D is not simulated either due to the lack of data or because the diffusive component of solute transport is assumed to be negligible in advection-dominated aquifers. These hydrogeological systems in fact represent the focus of the vast majority of hydrogeological research and practice. On the other hand, when groundwater flow velocities are low, such as in clay-rich formations characterized by low permeability, diffusion becomes a significant component of the transport process and in some cases is the dominant process (Cherry et al. 2007; Mazurek et al. 2011). In diffusion-dominated systems, the role of D on diffusive flux is similar to that of hydraulic conductivity on groundwater flow and therefore it is important to investigate the spatial distribution of D.

The spatial variability of D in clay-rich geological formations is the result of several physical and chemical factors acting at different scales. Main contributions to this variability are related to variations in the total connected porosity available to the diffusion process (accessible porosity), and to variations in the pore network geometry. The latter are caused by variability in the lengths of the diffusion paths (i.e., tortuosity) and in the pore width along the diffusion paths (i.e., constrictivity). Tortuosity and constrictivity are controlled by the distribution of bioclasts and detrital minerals between the clay matrix,

mineral content, mineral arrangement, grain-size distribution and sorting, and by diagenetic and consolidation histories. Mineral precipitation during diagenesis can decrease pore connectivity limiting the diffusion process, while an increase in the content of tectosilicates in the clay-rich matrix can enlarge the average pore size and decrease the tortuosity of the diffusion paths (Sammartino et al. 2003).

Alongside variations in the pore-network geometry, another important source of heterogeneity of D in clay-rich formations is the effect of interactions between chemical species in solutions and charged mineral surfaces. These interactions can be taken into account by the electrostatic constrictivity (e.g., Sato et al. 1994; Kato et al. 1995), which can be quantified according to the electric double-layer theory based on the Donnan equilibrium (Ochs et al. 2003; Revil and Linde 2006; Appelo and Wersin 2007; Jougnot et al. 2009; Appelo et al. 2010). This issue will be further discussed in Section 3.

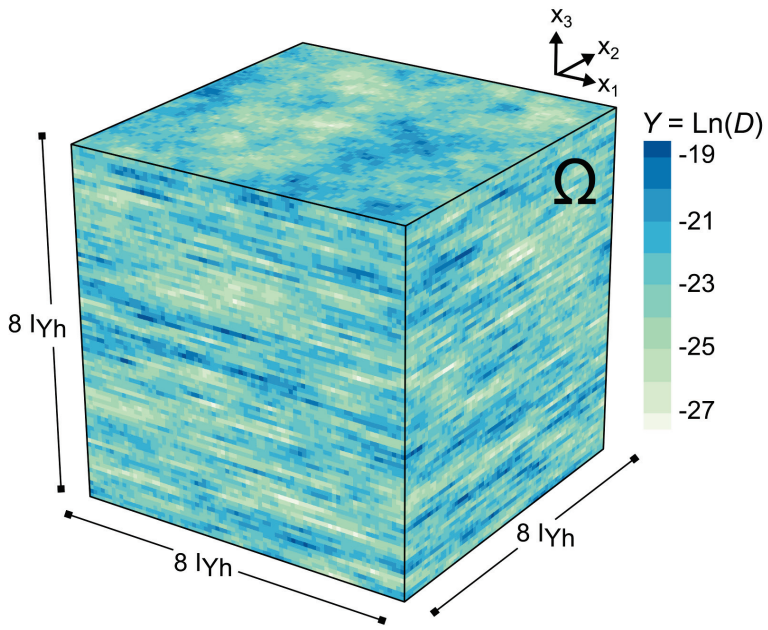

Figure 4. Three-dimensional cubic domain Ω with heterogeneous and anisotropic lognormal D field. In this realization, the variance of the distribution of the natural logarithm of D (σ_Y^2) is equal to 2.0 and the anisotropy ratio (I_{Yv}/I_{Yh}) is equal to 0.1.

2.2 Numerical experiments

2.2.1 Three-dimensional D fields

In this work, the heterogeneous and anisotropic spatial distribution of D is modeled with a geostatistical approach. We considered a three-dimensional cubic domain Ω characterized by a heterogeneous distribution of D (Figure 4) including all sources of spatial variability discussed in Section 2.1. We assumed that $D(\boldsymbol{x})$, where $\mathbf{x}(x_1, x_2, x_3)$ is a vector of Cartesian coordinates, is lognormal such that $Y(\boldsymbol{x}) = \mathrm{Ln}(D(\boldsymbol{x}))$ is a normal variate. The spatial distribution of $Y(\mathbf{x})$ can then be completely characterized by its mean $\langle Y \rangle$, variance σ_Y^2, and semivariogram function $\gamma(\boldsymbol{h})$, where $\boldsymbol{h}(h_1,h_2,h_3)$ is the separation distance vector between two arbitrary points in Ω. These parameters can be directly calculated from the geostatistical analysis of laboratory scale measurements in samples taken at different locations within the domain of interests. An axisymmetric exponential variogram model

$$\gamma(\boldsymbol{h}) = \sigma_Y^2 \left[1 - \exp\left(- \sqrt{\frac{{h_1}^2 + {h_2}^2}{{I_{Yh}}^2} + \frac{{h_3}^2}{{I_{Yv}}^2}} \right) \right] \quad (1)$$

was used to model the spatial variability of Y. I_{Yh} and I_{Yv} are the integral scales in the horizontal plane (x_1x_2) and in the vertical direction (x_3), respectively. The length of the side of Ω was set equal to 8 I_{Yh}. Spatial variability was assumed axisymmetric to take into account the layered structure of clay minerals and the bedding of clay-rich geological formations. Five σ_Y^2 values (0.1, 0.5, 1, 1.5 and 2) were assumed to represent different degrees of heterogeneity, while the geometric mean $\langle Y \rangle$ was kept constant. Generated fields were characterized by variations in D ranging from about one order of magnitude for σ_Y^2 equal to 0.1 up to about five orders of magnitude for fields with σ_Y^2 equal to 2. Three different values of the anisotropy ratio e ($I_{Yv}/I_{Yh} \leq 1$) were considered by varying I_{Yv} while I_{Yh} was kept constant. Geostatistical simulations of the spatial distribution of Y were performed with SGeMS (Remy et al. 2009), considering an interpolation grid with uniform spacing equal to $0.1I_{Yh}$.

2.2.2 Numerical estimation of the equivalent pore diffusion coefficient

Three-dimensional diffusive transport under steady state conditions was simulated by solving the mass balance equation:

$$\nabla \cdot [D(\boldsymbol{x}) \nabla C(\boldsymbol{x})] = 0 \quad (2)$$

The heterogeneous domain Ω was discretized into a finite-difference block-centered grid with the same resolution as the grid used for geostatistical simulations. Equation (2) was then solved numerically with the code MT3DMS v5.3 (Zheng 2010). Dirichlet (constant concentration) boundary conditions were applied to two opposite faces of Ω while no-mass-flux Neumann boundaries were applied to remaining faces. The resulting diffusive transport field has a spatially uniform mean component that is parallel to the Neumann boundaries.

The equivalent diffusion coefficient (D_{eq}) for direction i was calculated by applying Fick's first law between the Dirichelet boundaries:

$$D_{eq,i} = -\frac{Q_i \cdot L}{S \cdot \Delta C} \quad (3)$$

where Q_i is the total diffusive flux through Ω calculated from the numerical experiments, S is the area the cubic domain faces, and L and ΔC are the distance and the imposed concentration difference between Dirichlet boundaries, respectively. To calculate D_{eq} for directions parallel to the plane of maximum spatial correlation x_1x_2 (i.e., parallel to bedding planes of a hypothetical clay-rich geological formation) and normal to it, Dirichlet and Neumann boundaries were rotated accordingly. D_{eq} estimated with Equation (3) corresponds to the upscaled diffusion coefficient of a fictitious homogeneous system that can be assumed representative of the heterogeneous medium since the total diffusive fluxes through both systems, homogeneous and heterogeneous, are the same.

2.3 Analytical upscaling

2.3.1 Stochastic methods

Stochastic expressions estimate upscaled properties as a function of the statistics (i.e., $\langle Y \rangle$, σ_Y^2 and e) of the spatial random variable. These properties, called "effective" in the stochastic hydrogeology literature, are derived by averaging over an ensemble of realizations and, being independent of the macroscopic boundary conditions, are constant throughout the domain. For this reason they can be considered physically intrinsic properties of the medium. In the case of the D fields considered in this study, the stochastic "effective" diffusion coefficient (D_{eff}) was defined from an extension of Fick's first law by taking the mathematical expectations of the diffusive mass flux $q(\boldsymbol{x})$ and the concentration gradient (∇C):

$$E[q(\boldsymbol{x})] = -D_{eff}(\boldsymbol{x})\, E[\nabla C(\boldsymbol{x})] \tag{4}$$

where the notation E[ ] indicates mathematical expectation. To derive analytical expressions for D_{eff}, we applied the perturbation method and the spatial random function $Y(\boldsymbol{x})$ was decomposed into its mean $\langle Y \rangle$ and a zero-mean random perturbation $Y'(\boldsymbol{x})$:

$$Y(\boldsymbol{x}) = \langle Y \rangle + Y'(\boldsymbol{x}) \tag{5}$$

Since $Y = \mathrm{Ln}(D(\boldsymbol{x}))$, from the exponentiation of Equation (5) we have:

$$D(\boldsymbol{x}) = D_G \exp\big(Y'(\boldsymbol{x})\big) \tag{6}$$

where D_G is the geometric mean of the D field. Fick's first law can also be rewritten in terms of means and perturbations:

$$q(\boldsymbol{x}) = -D_G \left(1 + Y'(\boldsymbol{x}) + \frac{(Y'(\boldsymbol{x}))^2}{2} + \cdots\right) (\mathrm{E}[\nabla C(\boldsymbol{x})] + \nabla C'(\boldsymbol{x})) \tag{7}$$

where $\nabla C'(\boldsymbol{x})$ is a zero mean fluctuation of the concentration gradient around its expected value and the exponential term $\exp(Y'(\boldsymbol{x}))$ in Equation (6) has been expanded into a Taylor series. Taking the expected value:

$$E[q(\boldsymbol{x})] = -D_G \mathrm{E}\left[\left(1 + Y'(\boldsymbol{x}) + \frac{(Y'(\boldsymbol{x}))^2}{2} + \cdots\right) (\mathrm{E}[\nabla C(\boldsymbol{x})] + \nabla C'(\boldsymbol{x}))\right] \tag{8}$$

and by dropping terms beyond second order in perturbations (Gelhar 1993), we can calculate:

$$E[q(\boldsymbol{x})] = -D_G \left(\left(1 + \frac{\sigma_Y^2}{2}\right) \mathrm{E}[\nabla C(\boldsymbol{x})] + \mathrm{E}[Y'(\boldsymbol{x}) \nabla C'(\boldsymbol{x})]\right) \tag{9}$$

From the comparison between Equations (4) and (9) it is evident that in order to derive an expression for D_{eff}, the term $\mathrm{E}[Y'(\boldsymbol{x})\nabla C'(\boldsymbol{x})]$ has to be specified in terms of the mean gradient $\mathrm{E}[\nabla C(\boldsymbol{x})]$. For groundwater flow, this was solved by Gelhar and Axness (1983) for a hydraulic conductivity field with axisymmetric exponential correlation function. By applying this solution in the context of diffusive flow, we have:

$$\mathrm{E}[Y'(\boldsymbol{x})\nabla C'(\boldsymbol{x})] = -g_i \mathrm{E}[\nabla C(\boldsymbol{x})] \quad (10)$$

where g_i is a complex integral (Equation (51) in Gelhar and Axness 1983). Substituting Equation (10) into Equation (9) and rearranging, D_{eff} can then be calculated with the following expression:

$$D_{eff,i} = D_G\left(1 + \sigma_Y^2\left(\frac{1}{2} - g_i\right)\right) \quad (11)$$

For the particular case of a three-dimensional anisotropic medium characterized by an axisymmetric ($I_{Y1} = I_{Y2} > I_{Y3}$) spatial covariance function, the solutions of the integrals g_i can be expressed as a function of the anisotropy ratio e (Gelhar and Axness 1983):

$$g_1 = g_2 = 0.5\frac{e^2}{1-e^2}\left\{\left(e^2\sqrt{\frac{1-e^2}{e^2}}\right)^{-1}\tan^{-1}\left(\sqrt{\frac{1-e^2}{e^2}}\right) - 1\right\} \quad (12a)$$

$$g_3 = \frac{1}{1-e^2}\left\{1 - \left(\sqrt{\frac{1-e^2}{e^2}}\right)^{-1}\tan^{-1}\left(\sqrt{\frac{1-e^2}{e^2}}\right)\right\} \quad (12b)$$

The expression in Equation (11) is an approximated result since the perturbation expansion was truncated at the first-order of approximation in σ_Y^2. To take into account higher-order terms and generalize this result for larger σ_Y^2, the two terms within parenthesis in Equation (11) may be seen as the truncation of the Taylor expansion of an exponential function:

$$D_{eff,i} = D_G\exp\left(\sigma_Y^2\left(\frac{1}{2} - g_i\right)\right) \quad (13)$$

This assumption is known as the Landau-Lifshitz-Matheron conjecture. For isotropic media ($e \to 1$) $g_1 = g_2 = g_3 = 1/3$, so that:

$$D_{eff,i} = D_G\exp\left(\frac{\sigma_Y^2}{6}\right) \quad (14)$$

On the other hand, higher-order corrections term in σ_Y^2 can also be considered. De Wit (1995) provided the solution for a three-dimensional unbounded isotropic media including terms up to third-order in σ_Y^2. Applying this solution to our diffusive system we have:

$$D_{eff,i} = D_G\left(1 + \sigma_Y^2\left(\frac{1}{2} - \frac{1}{n}\right) + \frac{(\sigma_Y^2)^2}{2}\left(\frac{1}{2} - \frac{1}{n}\right)^2 + \frac{(\sigma_Y^2)^3}{6}\left(\frac{1}{2} - \frac{1}{n}\right)^3 + \delta\right) \quad (15)$$

where n is the number of space dimensions. The truncation error δ was evaluated numerically and for a Gaussian multivariate field characterized by an exponential spatial covariance it was found approximately equal to $-0.000467(\sigma_Y^2)^3$. Analogously, Indelmann and Abramovich (1994) investigated the problem of

calculating higher-order terms in anisotropic media. According to their solution, Equation (11) can be modified by including a second-order term in σ_Y^2:

$$D_{eff,i} = D_G\left(1 + \sigma_Y^2\left(\frac{1}{2} - g_i\right) + \frac{(\sigma_Y^2)^2}{2}\left(\left(\frac{1}{2} - g_i\right)^2 + \varepsilon_i\right)\right) \quad (16)$$

The truncation error ε_i is a six-dimensional integral (Equation (24) in Indelmann and Abramovich 1994) whose values depend on the shape of the spatial correlation function.

2.3.2 Power-averaging

Equivalent parameters can also be estimated by using a power-averaging formula. This approach, firstly introduced by Journel et al. (1986), was developed by Desbarats (1992) for calculating the equivalent hydraulic conductivity over a volume *V*. Applying this approach to the heterogeneous *D* fields, D_{eq} can be approximated with the following:

$$D_{eq} = \left[\frac{1}{\mathrm{V}}\int_V D(\boldsymbol{x})^p dV\right]^p \quad (17)$$

where the exponent *p* varies between -1 and +1. D_{eq} is equal to the harmonic mean (D_H) of the *D* field for p = -1 and to the arithmetic mean (D_A) for p = 1. The limit of D_{eq} as $p \rightarrow 0$ is equal to D_G. Using exponential expansions truncated to second-order terms, Desbarats (1992) developed a linear approximation of Equation (17) that is valid for multivariate Gaussian fields. Accordingly, D_{eq} can be estimated with the following expression:

$$D_{eq,i} = D_G \exp\left(\frac{1}{2}(\sigma_Y^2 - \bar{\gamma}(V) + \bar{\gamma}(V)p_i)\right) \quad (18)$$

The term $\bar{\gamma}(V)$ represents the ensemble variance of $Y(\boldsymbol{x})$ over the volume *V*. In general, as the length of the domain over which the ensemble variance is calculated increases, $\bar{\gamma}$ approximates the field variance σ_Y^2.

In our work, the averaging volume corresponds to the entire domain Ω and then D_{eq} for different directions *i* was estimated with the following expression:

$$D_{eq,i} = D_G \exp\left(\frac{\sigma_Y^2 p_i}{2}\right) \quad (19)$$

Parameter p_i was calculated by least-square fitting of Equation (19) to the D_{eq} values estimated with the numerical transport simulations. This parameter was also estimated using the analytical expression of Ababou (1991):

$$p_i = 1 - \frac{2}{n}\left[\frac{\left(\frac{1}{n}\sum_{i=1}^n {I_{Yi}}^{-1}\right)^{-1}}{I_{Yi}}\right] \quad (20)$$

2.4 Results

Numerically estimated D_{eq} values normalized by D_G are plotted in Figure 5, for different σ_Y^2 and e. In the isotropic case (e = 1), D_{eq} is the average of the values estimated for each of the coordinate directions x_1, x_2, x_3. For anisotropic cases (e≠1), $D_{eq,h}$ values correspond to the average of the values calculated in the horizontal plane (x_1x_2) while $D_{eq,v}$ represent equivalent values calculated in the x_3 direction. For each σ_Y^2, 350 realizations of the heterogeneous D field were generated. Therefore, each normalized D_{eq} was calculated by averaging the results from 350×3 numerical simulations in the isotropic case while 350×2 and 350 simulations were used to estimate $D_{eq,h}$ and $D_{eq,v}$, respectively.

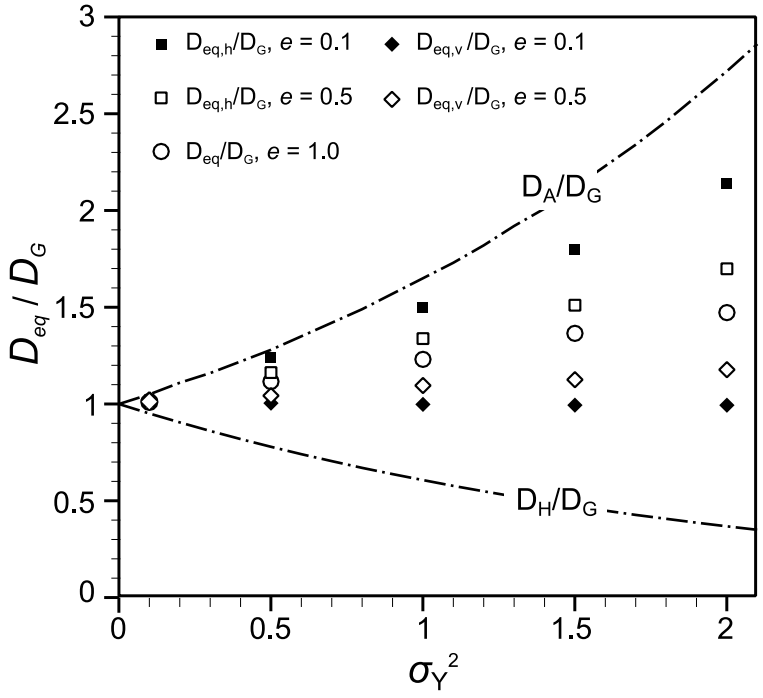

Figure 5. Numerically estimated equivalent D (D_{eq}), normalized by the geometric mean D_G, versus Ln(***D***) field variance (σ_Y^2) and different values of the anisotropy ratio e.

Several studies have shown that the equivalent hydraulic conductivity for any direction is bounded between the harmonic and the arithmetic means of the local hydraulic conductivity values (e.g., Cardwell and Parson 1945, Matheron 1967, Renard and de Marsily 1997). The two end-members represent equivalent values in a layered heterogeneous domain characterized by conditions of flow perpendicular and parallel to the layers, respectively. Our numerical results are within corresponding bounds (Figure 5). For a fixed σ_Y^2, as e decreases (higher anisotropy), the estimated $D_{eq,h}$ increases toward the limit represented by D_A, while $D_{eq,v}$ decreases and tends to D_H. It is expected that as $e \rightarrow 0$ the upscaled D_e values will tend toward their respective bounds. Our results suggest that for fields with moderate to low heterogeneity ($\sigma_Y^2 \leq 0.5$), the rates at which the equivalent values approach the bounds are faster than those of more heterogeneous fields. Morevover, as e decreases, the rate at which $D_{eq,h}$ reaches D_A is faster than the rate at which $D_{eq,v}$ reaches D_H.

Comparisons between numerically estimated D_{eq} values, normalized by D_G, and analytical predictions are shown in Figure 6. In particular, Figures 6a, 6b and 6c on the left side show the match between stochastic analytical expressions and numerical data for different values of e, whereas the power-averaging

expressions are in Figures 6d, 6e and 6f. Numerically estimated D_{eq} values can be compared with effective values from stochastic expressions since we considered a domain sufficiently large such that equivalent values approximate effective ones. In the case of parallel flow and isotropic spatial distribution of the random variable, the dimensional limit for this approximation to be valid is about four times the integral scale of the considered spatial random variable (Rubin and Dagan 1988; Paleologos et al. 2000; Sarris and Paleologos 2004). Since we considered a domain that is twice as large as this dimensional limit, we assume that equivalent and effective parameters are also comparable for the generated anisotropic fields. To quantify the mismatch between numerical and analytical values, the root mean square error (*RMSE*):

$$RMSE = \sqrt{\frac{1}{N}\sum\left(\frac{{D_{eq,i}}^{calc}}{D_G} - \frac{{D_{eq,i}}^{num}}{D_G}\right)^2} \tag{21}$$

and the mean absolute residual error (*MA*):

$$MA = \frac{1}{N}\sum\left|\frac{{D_{eq,i}}^{calc}}{D_G} - \frac{{D_{eq,i}}^{num}}{D_G}\right| \tag{22}$$

were calculated (Table 1). ${D_{eq,i}}^{calc}$ is the analytical prediction of D_{eq} for the direction i. Both *RMSE* and *MA* are statistical measures of the accuracy of the analytical expressions in predicting D_{eq} estimated through the numerical experiments (${D_{eq,i}}^{num}$). Better predictions are associated with *RMSE* and *MA* values that are closest to zero.

Table 1. RMSE and MA of the upscaling analytical expressions for different *D* fields.

Model	*e = 1.0*		*e = 0.5*				*e = 0.1*			
			$D_{eq,h}/D_G$		$D_{eq,v}/D_G$		$D_{eq,h}/D_G$		$D_{eq,v}/D_G$	
	MA	*RMSE*	*MA*	*RMSE*	*MA*	*RMSE*	*MA*	*RMSE*	*MA*	*RMSE*
Eq. 17	0.051	0.057	-	-	-	-	-	-	-	-
Eq. 17	0.052	0.058	-	-	-	-	-	-	-	-
Eq. 16	-	-	0.021	0.023	0.120	0.141	0.078	0.114	0.288	0.332
Eq. 18	-	-	0.077	0.114	0.034	0.036	0.262	0.366	0.104	0.113
Eq. 22[1]	0.013	0.014	0.017	0.019	0.006	0.007	0.021	0.023	0.004	0.006
Eq. 22[2]	0.051	0.057	0.041	0.044	0.092	0.108	0.055	0.080	0.271	0.312

[1] with fitted p_i
[2] analytical p_i

For isotropic fields (Figure 6a and 6c), both stochastic and power-averaging expressions are accurate for σ_Y^2 up to 1. At higher variances, both Equation (14), based on the Landau-Lifshitz-Matheron conjecture, and Equation (15), based on the third-order expression of De Wit (1995), slightly underestimate the

numerical D_{eq} values. Moreover, these two expressions are practically identical within the range of σ_Y^2 considered. On the other hand, the power-averaging expression with p_i calculated through least-square fitting of numerically estimated D_{eq} values is an excellent predictor of D_{eq} for any σ_Y^2. Since for $e = 1$ the analytical value of p_i calculated with Equation (20) is equal to 1/3, Equation (19) and Equation (14) provide identical results.

For anisotropic fields stochastic expressions are only partially accurate (Figure 6b and 6c). Equation (13) is a good approximation only when diffusive flow is parallel to the plane of maximum spatial correlation. Goodness-of-fit deteriorates with increasing σ_Y^2 and increasing anisotropy. On the other hand, $D_{eq,v}$ is largely underestimated in the range of anisotropy considered. This is shown by the *RMSE* and *MA* statistics whose values for the normalized $D_{eq,h}$ are more than 6 times ($e = 0.5$) and 3 times ($e = 0.1$) lower than those for predicted normalized $D_{eq,v}$. Interestingly, the opposite behavior is observed for the analytical predictions calculated with Equation (16). This expression in fact is more accurate than Equation (13) in predicting $D_{eq,v}$ rather than $D_{eq,h}$. Considering Equation (16), the *RMSE* for normalized $D_{eq,h}$ is equal to 0.114 for $e = 0.5$ and to 0.366 for $e = 0.1$. Conversely, the correspondent values for $D_{eq,v}$ are about 3 and 2.5 times lower. An analogous discrepancy in the accuracy of Equation (16) for predicting $D_{eq,h}$ and $D_{eq,v,}$ was detected by Sarris and Paleologos (2004) for the equivalent hydraulic conductivities in an anisotropic field. Our results imply that, for the range of σ_Y^2 considered, the Landau-Lifshitz-Matheron conjecture is appropriate only in systems where diffusive flow is parallel to layers while the fourth-order approximation of Equation (16) behaves just the opposite.

When p_i is calculated through least-square fitting, Equation (19) provides very accurate estimates of D_{eq} in anisotropic fields (Figure 6e and 6f). The maximum *RMSE* (0.023), corresponding to the normalized $D_{eq,h}$ in fields with $\sigma_Y^2 = 2$, is still lower than the *RMSE* of the most accurate prediction by any stochastic expression. An almost perfect match (*MA* and *RMSE* ≤ 0.006) is observed for anisotropic fields, especially for $D_{eq,v}$. On the other hand, the goodness-of-fit of Equation (19) when p_i is estimated analytically with Equation (20) (Ababou 1991) is similar to that of Equation (13), albeit Equation (19) with analytical p_i provides slightly more accurate estimates of $D_{eq,v}$. In terms of *RMSE*, the difference in accuracy between results with fitted and analytical p_i values is significant. On average, the *RMSE* of the predictions of normalized $D_{eq,h}$ made with the fitted p_i is about 3 times lower than with analytical p_i. This difference is even more evident for normalized $D_{eq,v}$ as shown by *MA* and *RMSE* values, which are 15 times lower in fields with $e = 0.5$ and up to more than 50 times lower in fields with $e = 0.1$. Fitted and analytical p_i values are compared in Table 2 where p_h and p_v represent p_i values estimated for normalized $D_{eq,h}$ and $D_{eq,h}$, respectively. The highest discrepancy between analytical and fitted p_i is observed for normalized $D_{eq,h}$.

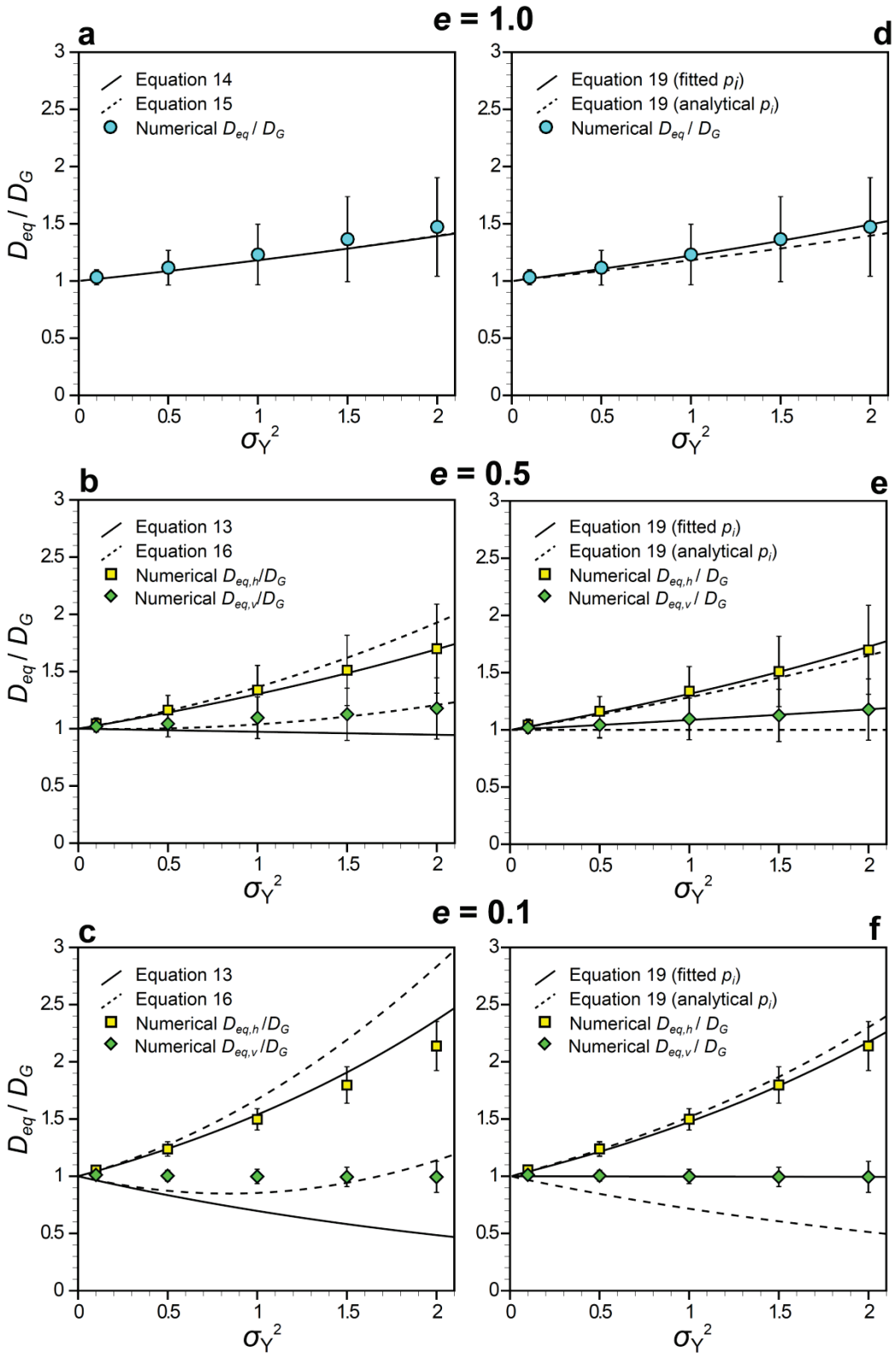

Figure 6. Comparison between numerical D_{eq} and analytical estimates.

Table 2. Analytical and least-square fitted values of the parameter p_i (Equation (19)).

e	*Fitted* p_h	*Analytical*[1] p_h	*Fitted* p_v	*Analytical*[1] p_v
0.1	0.776	0.833	-0.005	-0.667
0.5	0.546	0.500	0.165	0.000
1.0	0.401	0.333	0.401	0.333

[1] calculated with Equation (20).

2.5 Discussion

Useful insights into the range of applicability of different analytical expressions for upscaling D in clay-rich formations can be drawn from the results of this work. In media where the spatially varying D can be assumed statistically isotropic and characterized by a relatively low heterogeneity ($\sigma_Y^2 \leq 1$), both stochastic and power-averaging expressions can be effective for estimating D_{eq}, provided that the statistics (i.e., mean, variance and integral scale) of the D field are known. Published datasets of different clay-rich formations suggest that the variability at the centimetric to decimetric scale is typically small. These dimensions correspond to the support scale of most of the data since D is generally measured in laboratory diffusion experiments in rock samples. For example, D of ^{22}Na and ^{85}Sr in Opalinus Clay rock samples range from 1.20×10^{-11} m^2/s to 6.0×10^{-11} m^2/s for ^{22}Na and from 1.4×10^{-11} m^2/s to 2.4×10^{-11} m^2/s ^{85}Sr (Van Loon et al. 2004a, Van Loon et al. 2004b, Van Loon et al. 2005). Assuming a lognormal distribution, σ_Y^2 is 0.28 and 0.03 for ^{22}Na and ^{85}Sr, respectively. However, these data are representative of a very thin interval (15 cm) within the formation. At a larger scale, the variability of D_e may significantly increase. The variance σ_Y^2 of Ln(D) of tritiated water (HTO) measured at different depths in the Callovo-Oxfordian argillite is equal to 1.1. Measurements of D of iodide in the Boom Clay along a depth interval of about 100 m range between 9.1×10^{-11} m^2/s and 5.2×10^{-10} m^2/s, with an average value of 1.6×10^{-10} m^2/s and a standard deviation of 9.0×10^{-11} m^2/s (Huysmans and Dassargues 2006). Laboratory scale experiments also showed that D is anisotropic; Samper et al. (2008), for instance, found that the anisotropy ratio e of D for HTO in a cylindrical rock sample (30 cm high and 30 cm in diameter) of Callovo-Oxfordian argillite is between 0.26 and 0.56. In a Opalinus clay sample from Mont Terri (Switzerland), e was estimated to be equal to 0.25 for HTO and chloride (García-Gutiérrez et al. 2006).

Our analysis shows that a power-averaging expression with fitted p_i provides very accurate results in D fields characterized by high variability. This finding is consistent with the results of other studies in which a similar expression was applied to upscale hydraulic conductivity in a 3-D anisotropic heterogeneous domains (Sarris and Paleologos 2004; Zhang et al. 2010). However, the accuracy of this upscaling expression is dependent on finding proper values of p_i. At this point a general theoretical model for predicting p_i has not been proposed and its existence is questionable (Desbarats 1992). Our comparisons show that the analytical p_i values calculated with Equation (19) do not provide accurate predictions of D_{eq}. A bilinear expression where p_i is function of the normalized averaging block size and the anisotropy ratio e was also suggested (Equation (14) in Sarris and Paleologos 2004). Its application was tested for the considered domain but it was found that it does not match the fitted p_i values (Figure 7). It is possible that this mismatch is due to the relative smaller number of simulations considered by Sarris and Paleologos (2004), which led up to statistically less significant results compared to our work. On the other hand a linear relationship between p_i and e is also suggested by our results (plotted as dashed lines in Figure 7). The related results can be used to estimate upscaled diffusion coefficient values based on small-scale measurements. The upscaled values are then used in the related PA models.

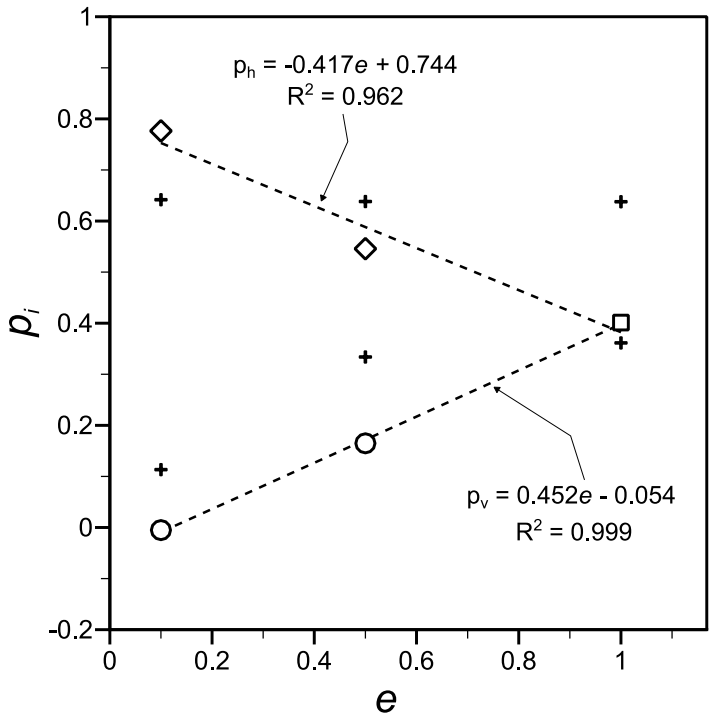

Figure 7. Values of fitted p_i as a function of e (diamonds: $\boldsymbol{p_h}$**;** circles: $\boldsymbol{p_v}$**;** square: p for isotropic fields). Black crosses corresponds to p_i calculated with equations proposed by Sarris and Paleologos 1994). R^2 is the coefficient of determination of the regressions lines (dashed).

3. EVALUATION OF THE FY11 MODEL CONSIDERING ELECTROCHEMICAL IMPACTS ON DIFFUSION IN CLAY-RICH GEOLOGICAL FORMATIONS

In FY11, we developed a new model that considers the effects of electrochemical interactions between ions and mineral surfaces by incorporating the dependence of D on the electrical properties of the clay rock (Zheng et al. 2011). The model conceptualizes pore water as divided into two parts: (1) mobile water in macropores that is not subject to electrochemical processes, and (2) pore water in the double-diffusion layer (DDL) that is strongly impacted by electrochemical processes. Based on the assumption that tortuosity and constrictivity and chemical potentials are the same for both macropore water and the DDL, Zheng et al. (2011) derived the following expression:

$$\frac{D_i}{D_M} = f + (1-f)exp\left[-\frac{z_i\varphi}{RT}\right] \quad (23)$$

where:

- D_i is the diffusion coefficient of the species *i;*
- D_M is the diffusion coefficient in the macropore space.
- f is the volumetric fraction of macropore water relative to the pore porosity;
- z_i is the charge number;
- R is the gas constant
- T is the absolute temperature;
- φ is the electrical potential.

The other assumption used in deriving Equation (23) is that φ is constant for a given formation. This assumption allows for significant simplification of the procedure to estimate the impacts of electrochemical processes, which is necessary for system-level PA models while more accurate consideration of electrochemistry may be needed in sub-process models (Rutqvist et al. 2012). This treatment will be evaluated as part of the evaluation of Equation (23).

The diffusion coefficient in the macropore space D_M can be calculated with the following expression:

$$D_M = \frac{D_{HTO}D_{w,i}}{D_{w,HTO}} \quad (24)$$

where D_{HTO} is the diffusion coefficient of for tritiated water (HTO) that is not subject to electrochemical interactions and subscript w refers to the diffusion coefficient in free water.

In our previous work Equation (23) was evaluated by comparing analytical predictions with few experimental data from the Opalinus Clay formation. In this work, we completed our previous evaluation by including all the data available in the literature for the Opalinus Clay. We also expanded evaluation by including also data collected in the Callovo-Oxfordian Argillites.

3.1 Data for model evaluation

The model represented by Equation (23) is evaluated by comparing analytical estimates with experimental diffusion coefficient values for different chemical species all of which available in the literature. In particular we focused on the Opalinus Clay (OPA) and Callovo-Oxfordian Argillites (COx)

since the majority of the data on diffusive parameters that is available in the literature were collected for these two geological formations. A summary of the sources considered for the data is presented in Table 3. The complete data set can be found in the report for the FY11 (Zheng et al. 2011)

In order to determine the diffusion-coefficient ratio D_i/D_M from the data, we calculated D_M with Equation (24), with the diffusion coefficient of HTO in free water and the diffusion coefficient of the chemical species determined from Harris and Woolf (1980) and Li and Gregory (1974). Since more than a single diffusion coefficient value was available for each chemical species, we took the average of all the available values considered for model evaluation (Figure 8a and 8c). We also carried out a separate computation of the average of all the values of chemical species having the same charge number (Figure 8b and 8d). For both clay-rich formations, the data for Cs^+ was not considered for model evaluations because of the high uncertainty of the experimental *D* values. This uncertainty may be caused by the fact that measured concentration or flux data used to determine diffusion coefficient estimates are not very sensitive to values for the diffusion coefficient for highly sorbed cations (Zheng et al. 2011).

Table 3. Chemical species considered for model evaluation and correspondent sources.

Chemical species	*References*	
	OPA	*COx*
Br^-	van der Kamp and Van Stempvoort (1998)	-
Cl^-	van der Kamp and Van Stempvoort (1998); Van Loon et al. (2003a); Van Loon et al. (2003b); Van Loon et al. (2004a); Garcia-Gutierrez et al. (2006)	Descostes et al. (2008)
Cs^{+1}	Maes et al. (2008)	Samper et al. (2008)
$H_2{}^{18}O$	van der Kamp and Van Stempvoort (1998)	-
HTO	Van Loon et al. (2003a); Van Loon et al. (2003b); Van Loon et al. (2004a); Van Loon et al. (2004b); Wersin et al. (2008)	Garcia-Gutierrez et al. (2008); Samper et al. (2008)
I^{-1}	Jefferies and Myatt (2000); Tevissen et al. (2004): Yllera et al. (2004); Van Loon et al. (2003a); Van Loon et al. (2003b); Van Loon et al. (2004a); Van Loon et al. (2004b); Wersin et al. (2008)	Descostes et al. (2008)
Na^+	Van Loon et al.(2004a); Van Loon et al. (2004b); Van Loon et al. (2005)	Garcia-Gutierrez et al. (2008);
Sr^{+2}	Van Loon et al. (2005)	Garcia-Gutierrez et al. (2008); Samper et al. (2008)

3.2 Model fitting

To calculate the diffusion coefficient ratio on the right hand side of Equation (23), the volumetric fraction of macropore water (f) and the electrical potential (φ) were considered as to be fitting parameters. This is justified by the fact that an acceptable approach for estimating these two parameters independently from relevant data is not yet available in the literature. On the other hand, the absolute temperature (T) was considered as constant and equal to 298.15 K. This assumption was tested by conducting a sensitivity analysis, which showed that Equation (23) is not sensitive to T within the range of temperatures at which the diffusion coefficient data were measured. The optimal values of f and φ were estimated with a nonlinear least-squares routine in Octave 3.6.2, which implements the Levenberg-Marquardt method to minimize the sum of the squares of the weighted residuals between the measured diffusion coefficient ratios (D_i/D_M) and the predictions from Equation (23). For each chemical species, the weights used in the optimization algorithm correspond to the reciprocal of the variances of the measured values.

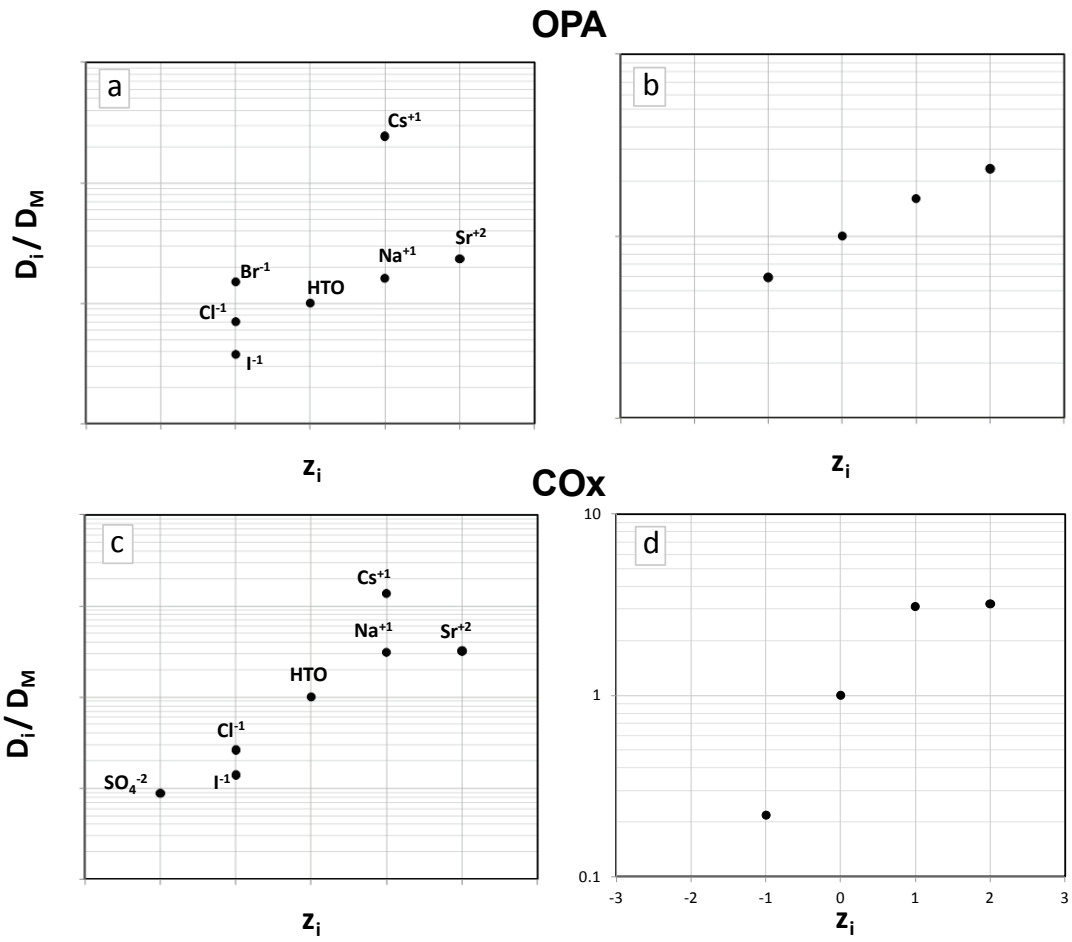

Figure 8. Experimental values of the ratio D_i/D_M for different values of the change number z_i. Points in Figure 8a and Figure 8c represent the average values of the experimental data for each chemical species considered. Points in Figure 8b and Figure 8d represent the average values of all experimental data of chemical species having the same charge number.

3.3 Comparison with experimental data

Comparisons between the measured ratio and the best match of Equation (23) to the data are presented in Figure 9. The optimal values of the fitting parameters and the values for the coefficient of determination R^2 are presented in Table 4. For all the data considered, these optimal values correspond to the unique minimum of the objective function previously described (Figure 10).

With respect to the Opalinus Clay data (Figure 9a and Figure 9b), the model represented in Equation (23) provides a very good match between measured and estimated values. This is especially evident when we fitted the model to the average values of the ratio D_i/D_M of chemical species with the same charge number ($R^2 = 0.995$). The optimal values for the fitting parameters f and φ are equal to 0.0 and about -11 mV. Unfortunately, for the OPA, there are not yet available data for this parameter that can be used to evaluate the physical consistency of our estimation.

Table 4. Model fitting results.

Geological formation	*Data type*	*f*	*Φ (mV)*	*R²*
OPA	Average *D* for each species (Figure 8a)	0.0	-11.1	0.686
	Average *D* for each charge number (Figure 8b)	0.0	-11.0	0.995
COx	Average *D* for each species (Figure 8c)	0.0	-23.3	0.254
	Average *D* for each charge number (Figure 8d)	0.0	-20.0	0.657

When compared to the COx data, Equation (23) is a less accurate predictor of the experimental data. However, the largest mismatch between observed and calculated ratio values is associated with Sr^{2+} (the only cation with charge number z_i equal to 2 in Figures 9a and 9b) for which the available data shows the highest uncertainty. In particular, the measured ratio D_i/D_M ranges between about 2.7 and about 4.3 according to two different data sources (Samper et al. 2008 and Garcia-Gutierrez et al. 2008, respectively). Not considering the Sr^{2+} data significantly improves the match between observed and estimated values. When all the chemical species are considered in the fitting procedure, optimal value for the electrical potential in the COx formation is between -20.0 and – 23.3 mV. When Sr^{2+} data is not taken into account, the optimal electrical potential is about -34 mV. These results are comparable to the electrical potential values estimated in the COx available in the literature. In particular, Jougnot et al. (2009) compared a model in which the electrical potential is a fitting parameter to tracer through-diffusion experiments in COx samples. By considering three different tracers ($^{22}Na^+$, $^{36}Cl^-$ and $^{35}SO_4^{2-}$), the optimal values for the electrical potential was found in the range from -23.8 mV to-47.0 mV. Interestingly, as for the OPA data, the optimal value for the fraction of macropore water f is zero. While a further refinement of Equation (23) and associated evaluation based on the data sets is on-going, it is important to note that f=0 means that all the pore water in clay pore space is in double-diffusive layer. This highlights the need to accurately consider electrochemical processes in modeling diffusion in clay formations.

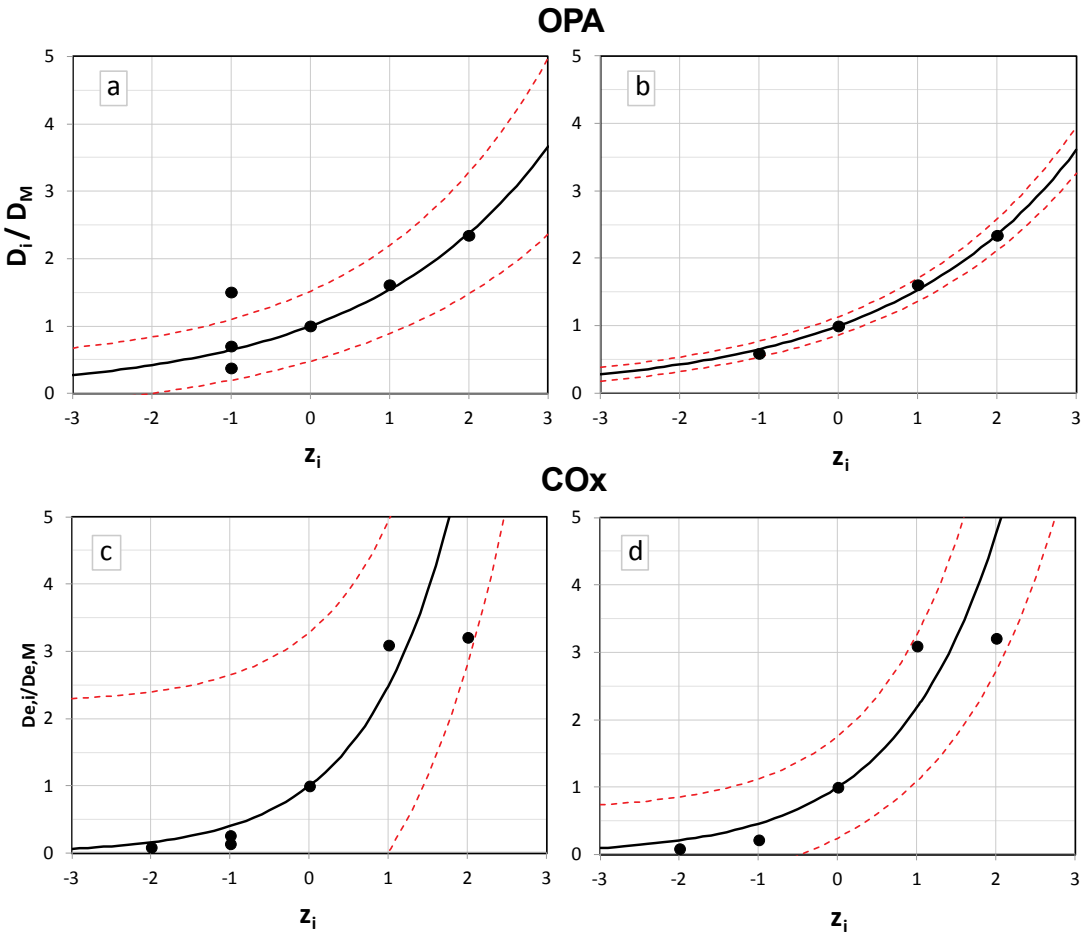

Figure 9. Comparison between calculated (black lines) and observed (circles) values for the ratio D_i/D_M for different values of the change number z_i. Red lines represent the 90% confidence intervals of the regression lines.

4. CONCLUDING REMARK AND FUTURE WORK

The dominant transport process in clay-rich geological formations is diffusion. Consequentially, modeling diffusive transport is important for the performance assessment of clay repositories. However, modeling diffusion in clay is complicated by the existence of heterogeneity at different scales and coupling between diffusive and electro-chemical processes. This report describes a study aimed at improving our understanding about how to effectively model diffusive transport in clay-rich formations. Our FY12 accomplishments include:

- We have developed a rigorous and practical framework for incorporating the impact of heterogeneity on diffusion processes in clay formations. This development is based on the analogy between diffusion and water flow in saturated heterogeneous porous media. The latter has been intensively investigated in the past two decades.
- We have evaluated a simplified approach to incorporating electrochemical impacts on diffusion in clay that was developed in FY11. Preliminary evaluation results are positive.

Specifically, the following conclusions can be drawn from this study:

- Conventional stochastic and power-averaging upscaling methods, originally developed for hydraulic conductivity fields, can be effectively applied to upscale laboratory-scale D measurements and to estimate representative input parameters for large scale numerical models.
- In media characterized by low heterogeneity (i.e., $\sigma_Y^2 \leq 1$), both stochastic and power-averaging expressions provide accurate estimates of D_{eq}. This conclusion is valid independent of the values of the anisotropy ratio e.
- In fields characterized by higher heterogeneity, stochastic expressions are less accurate than power-averaging methods especially in anisotropic fields ($e \neq 1$). In particular, we evaluated two stochastic anisotropic expressions, with both showing discrepancies in terms of accuracy when used to upscale D for mass diffusion parallel or perpendicular the layers. Our results suggest that the Landau-Lifshitz-Matheron conjecture is only accurate when mass diffusion is parallel to the layering while a fourth-order approximation behaves just the opposite.
- Within the range of heterogeneity and anisotropy considered, the power-averaging expression of Equation (19) provides accurate estimates of D_{eq} when parameter p_i is estimated by fitting numerical results. Less accurate predictions, comparable to those from stochastic methods, are obtained when p_i is calculated analytically.
- Results show linear dependency between p_i and e, and two linear expressions are suggested to calculate p_h and p_v as function of e.
- There is a good match between analytical predictions based on Equation (23) and measured data, especially for the Opalinus Clay.
- Two parameters in Equation (23) were considered as fitting parameters. These include the fraction of macropore water and the electrical potential. The latter parameter was estimated equal to about -11 mV in the Opalinus Clays and to about -23 mV in the Callovo-Oxfordian Argillites.
- For both of the geological formations under consideration, the optimal values for the macropore water fraction are zero, suggesting that the entire pore space is occupied by the DDL and therefore subject to electrochemical processes.

In the remaining months of FY12, we will:

- Continue to evaluate our approach for incorporating the impacts of electrochemical processes. In particular we will focus on the physical meaning and uncertainties of the estimated parameter values (f and φ).

In FY13, we propose to:

- Build on the current study to develop a framework for estimating the uncertainty of upscaled diffusion coefficients by incorporating measurement errors, uncertainty in estimating the statistical parameters of the local scale diffusion coefficient (e.g., variance and correlation length), and uncertainty in simplifying electrochemical processes.
- Integrate this activity with the system-level clay model developed by ANL by providing inputs (upscaled parameter values and related uncertainty) to the ANL model.

5. REFERENCES

Ababou, R. 1991. *Identification of effective conductivity tensor in randomly heterogeneous and stratified Aquifers.* In S. Bachu (Ed.) Proceedings of the 5th Canadian/American Conference on hydrogeology: parameter identification and estimation for aquifer and reservoir characterization: National Well Water Association, Dublin, Ohio: 155-157.

Aertsens, M., I. Wemaere and L. Wouters 2004. *Spatial variability of transport parameters in the Boom Clay*. Applied Clay Science 26: 37–45.

ANDRA 2005. *Dossier 2005 Référentiel du site Meuse/Haute-Marne*. Rapport Andra n° C RP ADS 04-0022.

Appelo, C. A. J. and P. Wersin 2007. *Multicomponent diffusion modeling in clay systems with application to the diffusion of tritium, iodide, and sodium in opalinus clay*. Environmental Science & Technology 41: 5002–5007.

Appelo, C.A.J., L.R. Van Loon and P. Wersin P. 2010. *Multicomponent diffusion of a suite of tracers (HTO, Cl, Br, I, Na, Sr, Cs) in a single sample of Opalinus Clay*. Geochimica et Cosmochimica Acta 74(4): 1201-1219.

Barnichon, J.D. and G. Volckaert 2003. *Observations and Predictions of Hydromechanical Coupling Effects in the Boom Clay, Mol Underground Research Laboratory, Belgium*. Hydrogeology Journal 11(1): 193-202.

Bossart, P., P. Meier, A. Möri, T. Trick and J.-C. Mayor 2001. *Geological and hydraulic characterization of the excavation disturbed zone in the Opalinus Clay of the Mont Terri Rock Laboratory*. Engineering Geology 66: 19-38.

Boving, T.B. and P. Grathwohl 2001. *Tracer diffusion coefficients in sedimentary rocks: correlation to porosity and hydraulic conductivity*. Journal of Contaminant Hydrology 53: 85–100.

Bradbury, K.R., M.G. Gotkowitz, J.A. Cherry, D. J. Hart, T.T. Eaton, B.L. Parker and M.A. Borchardt 2007. *Contaminant Transport Through Aquitards: Technical Guidance for Aquitard Assessment*. Awwa Research Foundation, Report 91133B, Denver, Colorado: 143.

Cardwell, W. T., and R. L. Parsons 1945. *Averaging permeability of heterogeneous oil sands*. Transactions. American Institute of Mining, Metallurgical and Petroleum Engineers 160: 34–42.

Cherry, J.A., B.L. Parker, K.R. Bradbury, T.T. Eaton, M.G. Gotkowitz, D.J. Hart and M.A. Borchardt 2007. *Contaminant Transport Through Aquitards: A State of the Science Review*. Awwa Research Foundation, Report 91133A. Denver, Colorado: 126.

Churakov, S. and T. Gimmi 2011. *Up-scaling of molecular diffusion coefficients in clays: a two-step approach*. The Journal of Physical Chemistry C 115(14): 6703-6714.

Cormenzana, J.L., M. García-Gutiérrez, T. Missana and Ú. Alonso 2008. *Modelling large-scale laboratory HTO and strontium diffusion experiments in Mont Terri and Bure clay rocks.* Physics and Chemistry of the Earth 33(14–16): 949-956.

Dagan, G. 1984. *Solute transport in heterogenous porous formations*. The Journal of Fluid Mechanics 145: 151–177.

Dagan, G. 1988. *Time-dependent macrodispersion for solute transport in anisotropic heterogeneous aquifers*. Water Resources Research 24(9): 1491–1500.

Dai, Z., A. Wolfsberg, Z. Lu and P. Reimus 2007. *Upscaling matrix diffusion coefficients for heterogeneous fractured rocks.* Geophysical Research Letters 34 L07408: doi:10.1029/2007GL029332.

Desbarats, A. J. 1992. *Spatial averaging of hydraulic conductivity in three-dimensional heterogeneous porous media.* Mathematical Geology 24(3): 249-267.

Descostes, M., V. Blin, F. Bazer-Bachi, P. Meier, B. Grenut, J. Radwan, M.L. Schlegel, S. Buschaert, D. Coelho E. and Tevissen 2008. *Diffusion of anionic species in Callovo-Oxfordian argillites and Oxfordian limestones (Meuse/Haute–Marne, France)*. Applied Geochemistry 23: 655–677.

De Wit, A. 1995. *Correlation structure dependence of the effective permeability of heterogeneous porous-media*. Physics of Fluids 7(11): 2553–2562.

Frippiat, C. and A.E. Holeyman 2008. *A comparative review of upscaling methods for solute transport in heterogeneous porous media*. Journal of Hydrology 362(1–2): 150-176.

Indelman, P, and B. Abramovich 1994a. *A higher-order approximation to effective conductivity in media of anisotropic random structure*. Water Resources Research 30(6): 1857–1864.

García-Gutiérrez, M., J.L. Cormenzana, T. Missana, M. Mingarro and P.L. Martín 2006. *Large-scale laboratory diffusion experiments in clay rocks*. Physics and Chemistry of the Earth 31: 523–530.

García-Gutiérrez, M., J.L. Cormenzana, T. Missana, M. Mingarro, U. Alonso, J. Samper, Q. Yang and S. Yi 2008. *Diffusion experiments in Callovo-Oxfordian clay from the Meuse/Haute-Marne URL, France. Experimental setup and data analyses.* Physics and Chemistry of the Earth, Parts A/B/C (33) Supplement 1: S125-S130.

Gelhar, L. W., A. L. Gutjahr and R. L. Naff 1979. *Stochastic analysis of macrodispersion in a stratified aquifer*. Water Resources Research 15(6): 1387–1397.

Gelhar, L. W. and C. L. Axness 1983. *Three-dimensional stochastic analysis of macrodispersion in aquifers*. Water Resources Research 19(1): 161–180.

Gonzales, S. and K.S. Johnson 1984. *Shale and other argillaceous strata in the United States.* Oak Ridge National Laboratory. ORNL/Sub/84-64794/1.

Harris, K.R. and L. A. Woolf 1980. *Pressure and Temperature Dependence of the Self Diffusion Coefficient of Water and Oxygen-18 Water*. J.C.S. Faraday I 76: 377-385

Huysmans, M. and A. Dessargues 2006. *Stochastic analysis of the effect of spatial variability of diffusion parameters on radionuclide transport in a low permeability clay layer*. Hydrogeology Journal 14: 1094–1106.

Huysmans, M. and A. Dessargues 2007. *Equivalent diffusion coefficient and equivalent diffusion accessible porosity of a stratified porous medium*. Transport in Porous Media 66(3): 421-438.

Indelman, P. and B. Abramovich 1994. *A higher-order approximation to effective conductivity in media of anisotropic random structure*. Water Resources Research 30(6): 1857–1864

Jefferies, N.L. and B.J. Myatt 2000. *Laboratory experiment on an Opalinus clay sample*. Mont Terri Project Technical Note, TN 99-61, Switzerland.

Jougnot, D., A. Revil and P. Leroy 2009. *Diffusion of ionic tracers in the Callovo-Oxfordian clay-rock using the Donnan equilibrium model and the electrical formation factor*. Geochimica et Cosmochimica Acta 73: 2712–2726.

Journel, A. G., C. V. Deutsch and A. J. Desbarats 1986. *Power averaging for block effective permeability.* Paper presented at 56th California Regional Meeting, Soc. of Pet. Eng., Oakland, California.

Li, Y. H. and S. Gregory 1974. *Diffusion of ions in seawater and deep sea sediments*. Geochimica et Cosmochimica Acta 38: 708-714.

Maes, N., S. Salah, D. Jacques, M. Aertsens, M. Van Gompel, P. De Cannière and N. Velitchkova 2008. *Retention of Cs in Boom Clay: Comparison of data from batch sorption tests and diffusion experiments on intact clay cores.* Physics and Chemistry of the Earth, Parts A/B/C 33(Supplement 1): S149-S155.

Matheron, G. 1967. *Elements pour une Théorie des Miliéux Poruex*, Masson, Paris.

Mazurek, M., P. Alt-Epping, A. Bath, T. Gimmi, N.H. Waber, S. Buschaert, P. De Cannière, M. De Craen, A. Gautschi, S. Savoye, A. Vinsot, I. Wemaere and L. Wouters 2011. *Natural tracer profiles across argillaceous formations.* Applied Geochemistry 6 (7): 1035–1064

NAGRA 2002. *Project Opalinus Clay: safety report. Demonstration of disposal feasibility for spent fuel, vitrified high-level waste and long-lived intermediate level waste (Entsorgungsnachweis)*. Nagra Technical Report NTB 02-05, Wettingen, Switzerland.

Neuman, S. P., C. L. Winter and C. M. Newman 1987. *Stochastic theory of field-scale Fickian dispersion, in ansiotropic porous media.* Water Resources Research 23(3): 453–466.

Ochs ,M., B. Lothenbach , M. Shibata, H. Sato and M. Yui 2003. *Sensitivity analysis of radionuclide migration in compacted bentonite: a mechanistic model approach.* Journal of Contaminant Hydrology 61(1–4): 313-328.

Paleologos, E.K., T. Sarris and A. Desbarats 2000. *Numerical estimation of effective hydraulic conductivity in leaky heterogeneous aquitards*. GSA Special Volume: ‘‘Theory, Modeling and Field Investigation in Hydrogeology: A Special Volume in Honor of Shlomo P. Neuman’s 60th Birthday’’: 119–127.

Patriarche, D., J.-L. Michelet, E. Ledoux and S. Savoye 2004. *Diffusion as the main process for mass transport in very low water content argillites: 1. Chloride as a natural tracer for mass transport—Diffusion coefficient and concentration measurements in interstitial water.* Water Resources Research 40(1): W01517, doi:10.1029/2003WR002700.

Remy, N., A. Boucher and J. Wu 2009. *Applied Geostatistics with SGeMS: A User’s Guide*. New York, Cambridge University Press: 264

Renard, P. and G. de Marsily 1997. *Calculating equivalent permeability: a review*. Advances in Water Resources 20: 253–278.

Revil, A. and N. Linde 2006. *Chemico-electromechanical coupling in microporous media.* Journal of Colloid and Interface Science 302: 682–694.

Rubin, Y. 1990. *Stochastic modeling of macrodispersion in heterogeneous porous media.* Water Resources Research 26(1): 133–141.

Rubin, Y. and G. Dagan 1988. S*tochastic analysis of boundaries effects on head spatial variability in heterogeneous aquifers, 1: constant head boundary*, Water Resources Research 24(10): 1689–1697.

Rutqvist, J., C. Steefel, J. Davis, I. Bourg, R. Tinnacher, J. Galindez, M. Holmboe, J. Birkholzer, and H.H. Liu 2012. *Investigation of reactive transport and coupled THM processes in EBS: FY12 report.* FCRD-UFD-2012-000125. US Department of Energy.

Sammartino, S., A. Bouchet, D. Prêt, J.C. Parneix and E. Tevissen 2003. *Spatial distribution of porosity and minerals in clay rocks from the Callovo-Oxfordian formation (Meuse/Haute-Marne, Eastern France) – implications on ionic species diffusion and rock sorption capability*. Applied Clay Science 23: 157–166.

Samper, J., Q. Yang, S. Yi, M. García-Gutiérrez, T. Missana, M. Mingarro, Ú. Alonso and J.L. Cormenzana 2008. *Numerical modelling of large-scale solid-source diffusion experiment in Callovo-Oxfordian clay.* Physics and Chemistry of the Earth 33 (Suppl. 1): S208–S215.

Sanchez-Vila, X., A. Guadagnini, and J. Carrera 2006. *Representative hydraulic conductivities in saturated groundwater flow.* Reviews of Geophysics 44: RG3002, doi:10.1029/2005RG000169.

Sarris, T., and E.K. Paleologos 2004. *Numerical Investigation of the Anisotropic Hydraulic Conductivity Behavior in Heterogeneous Porous Media.* Stochastic Environmental Research and Risk Assessment 18: 188-197.

Sato, H., M. Yui and H. Yoshikawa 1994. *Diffusion Behavior for Se and Zr in Sodium-Bentonite*. MRS Proceedings 353: 269-353.

Van der Kamp, G. and D. R. Van Stempvoort 1998. *Water sampling (laboratory) experiment (WS-B). Laboratory measurement of porosity, pore water isotopic composition and effective diffusivities of Opalinus Clay core samples*. Mont Terri Project, Technical Note 99-38, 1998.

Van Loon, L. R., J. M. Soler and M. H. Bradbury 2003a. *Diffusion of HTO, $^{36}Cl^-$ and $^{125}I^-$ in Opalinus Clay samples from Mont Terri: Effect of confining pressure*. Journal of Contaminant Hydrology 61(1-4): 73-83.

Van Loon, L. R., J. M. Soler, A. Jakob and M. H. Bradbury 2003b. *Effect of confining pressure on the diffusion of HTO, $^{36}Cl^-$ and $^{125}I^-$ in a layered argillaceous rock (Opalinus Clay): diffusion perpendicular to the fabric*. Applied Geochemistry 18(10): 1653-1662.

Van Loon, L.R., J.M. Soler, W. Muller and M.H. Bradbury 2004a. *Anisotropic diffusion in layered argillaceous rocks: a case study with opalinus clay.* Environmental Science & Technology 38: 5721–5728.

Van Loon, L.R., P. Wersin, J.M. Soler, J. Eikenberg, T. Gimmi, P. Hernan, S. Dewonck and S. Savoye 2004b. *In-situ diffusion of HTO, $^{22}Na^+$, Cs^+ and I^- in Opalinus Clay at the Mont Terri underground rock laboratory*. Radiochimica Acta 92: 757–763.

Van Loon, L.R., B. Baeyens and M.H. Bradbury 2005. *Diffusion and retention of sodium and strontium in Opalinus clay: Comparison of sorption data from diffusion and batch sorption measurements, and geochemical calculations*. Applied Geochemistry 20: 2351-2363.

Van Marcke, Ph. And B. Laenen 2005. *The Ypresian Clays as Possible Host Rock for Radioactive Waste Disposal: An Evaluation*. ONDRAF/NIRAS, Brussel.

Wen, X.-H. and J. Gómez-Hernández 1996. *Upscaling hydraulic conductivities in heterogeneous media: An overview*. Journal of Hydrology 183 (1–2): ix-xxxii.

Yllera, A., A. Hernandez, M. Mingarro, A. Quejido, L.A. Sedano, J.M. Soler, J. Samper, J. Molinero, J.M. Barcala, P.L. Martin, M. Fernandez, P. Wersin, P. Rivas and P. Hernan 2004. *DI-B experiment: planning, design and performance of an in situ diffusion experiment in the Opalinus clay formation*. Applied Clay Science 26: 181-196.

Zhang, D. and S. P. Neuman 1996. *Effect of local dispersion on solute transport in randomly heterogeneous media*. Water Resources Research 32(9): 2715– 2723.

Zhang, Y., C. W. Gable and B. Sheets B. 2010. *Equivalent hydraulic conductivity of three-dimensional heterogeneous porous media: An upscaling study based on an experimental stratigraphy*. Journal of Hydrology 388(3–4): 304-320.

Zheng, C. 2010. *MT3DMS v5.3 a modular three-dimensional multispecies transport model for simulation of advection, dispersion and chemical reactions of contaminants in groundwater systems.* Supplemental User's Guide, Technical Report to the U.S. Army Engineer Research and Development Center, Department of Geological Sciences, University of Alabama, 51 p.

Zheng, L., H.H. Liu, J. Birkoltzer and W.M. Nutt 2011. *Diffusion modeling in a generic clay repository.* FCRD-LBNL-2011-SLM: 25

Zhou, L., and H.M. Selim 2003. *Scale-dependent dispersion in soils: an overview*. Advances in Agronomy 80: 223–263.